JKMS

Original Article
Biomedical Engineering

Check for updates

Proarrhythmogenic Effect of the L532P and N588K *KCNH2* Mutations in the Human Heart Using a 3D Electrophysiological Model

Aulia Khamas Heikhmakhtiar (ID),[1,2] **Abebe Tekle Abrha** (ID),[3] **Da Un Jeong** (ID),[3] **and Ki Moo Lim** (ID) [3]

[1]School of Computing, Telkom University, Bandung, Jawa Barat, Indonesia
[2]Research Center of Human Centric Engineering (HUMIC), Telkom University, Bandung, Jawa Barat, Indonesia
[3]Department of IT Convergence Engineering, Kumoh National Institute of Technology, Gumi, Korea

 OPEN ACCESS

ORCID iDs
Aulia Khamas Heikhmakhtiar (ID)
https://orcid.org/0000-0001-9452-4064
Abebe Tekle Abrha (ID)
https://orcid.org/0000-0002-5332-3546
Da Un Jeong (ID)
https://orcid.org/0000-0001-8490-5007
Ki Moo Lim (ID)
https://orcid.org/0000-0001-6729-8129

ABSTRACT

Background: Atrial arrhythmia is a cardiac disorder caused by abnormal electrical signaling and transmission, which can result in atrial fibrillation and eventual death. Genetic defects in ion channels can cause myocardial repolarization disorders. Arrhythmia-associated gene mutations, including *KCNH2* gene mutations, which are one of the most common genetic disorders, have been reported. This mutation causes abnormal QT intervals by a gain of function in the rapid delayed rectifier potassium channel (I_{Kr}). In this study, we demonstrated that mutations in the *KCNH2* gene cause atrial arrhythmia.
Methods: The N588K and L532P mutations were induced in the Courtemanche-Ramirez-Nattel (CRN) cell model, which was subjected to two-dimensional and three-dimensional simulations to compare the electrical conduction patterns of the wild-type and mutant-type genes.
Results: In contrast to the early self-termination of the wild-type conduction waveforms, the conduction waveform of the mutant-type retained the reentrant wave (N588K) and caused a spiral break-up, resulting in irregular wave generation (L532P).
Conclusion: The present study confirmed that the *KCNH2* gene mutation increases the vulnerability of the atrial tissue for arrhythmia.

Keywords: *KCNH2* Gene Mutation; L532P Mutation; N588K Mutation; Three-dimensional Heart Modeling

INTRODUCTION

Heart failure has been a major cause of death worldwide for the past few decades. Arrhythmia, one of the causes of heart failure, is characterized by an abnormal rhythm of the heartbeat and is caused by dyssynchronous ion exchange or current in myocardial cells resulting from genetic mutations in protein channels.[1,2] Prolonged persistence of arrhythmia can alter the excitation and contraction sequences to cause fibrillation[3] and even death because blood cannot be ejected effectively.[4,5] Short QT syndrome is one cause subject to arrhythmia due to genetic mutation in the ionic channel.

Author Contributions

Conceptualization: Lim KM. Data curation: Heikhmakhtiar AK, Jeong DU, Abrha AT. Formal analysis: Heikhmakhtiar AK, Jeong DU, Abrha AT. Investigation: Heikhmakhtiar AK, Jeong DU, Abrha AT. Methodology: Lim KM. Software: Lim KM. Validation: Lim KM. Writing - original draft: Heikhmakhtiar AK, Jeong DU, Abrha AT. Writing - review & editing: Lim KM.

Short QT syndrome is described by the time interval of Q to T wave of the electrocardiogram (ECG) is less than 300 msec.[6] The first identification of short QT syndrome was described by Gussak et al.[7] The short QT syndrome increased arrhythmia generation because it shortened the refractory period, which prone to reentry resulting in chaotic electrical activity in the heart. Giustetto et al.[8] stated that short QT syndrome is a rare condition because of a limited number of patients reported in published data, however, may play a role in sudden infant death. N588K *KCNH2* is the first protein with a genetic mutation to be discovered in patients with short QT syndrome.[6,9] In 2011, Zhang et al.[10] performed an experimental study of L532P *KCNH2* mutation which associates with short QT as the comparative subject with N588K mutation.

The *KCNH2* mutation affects the alpha-subunit of the rapid delayed rectifier potassium channel (I_{Kr}) that plays a role in repolarization (**Fig. 1A**).[6,11,12] This gene can regulate changes in voltage activation in the heart and nervous tissue and is known to fasten cardiac repolarization by a gain of function and associated with short QT syndrome. N588K and L532P—the genetic mutations of *KCNH2*—are known to induce atrial arrhythmia. N588K is a fibril-related gain-of-function mutation in which the negatively charged asparagine (N) of residue N588 at the outer entrance of the *KCNH2* channel subunit (S5) is replaced with the positively charged lysine (K) (**Fig. 1B**).[9] In the L532P mutation, the leucine (L) of residue L532 located in the voltage sensor (S4) of the *KCNH2* channel is replaced with proline (P) (**Fig. 1B**).[13] L532P mutation is located in a different segment
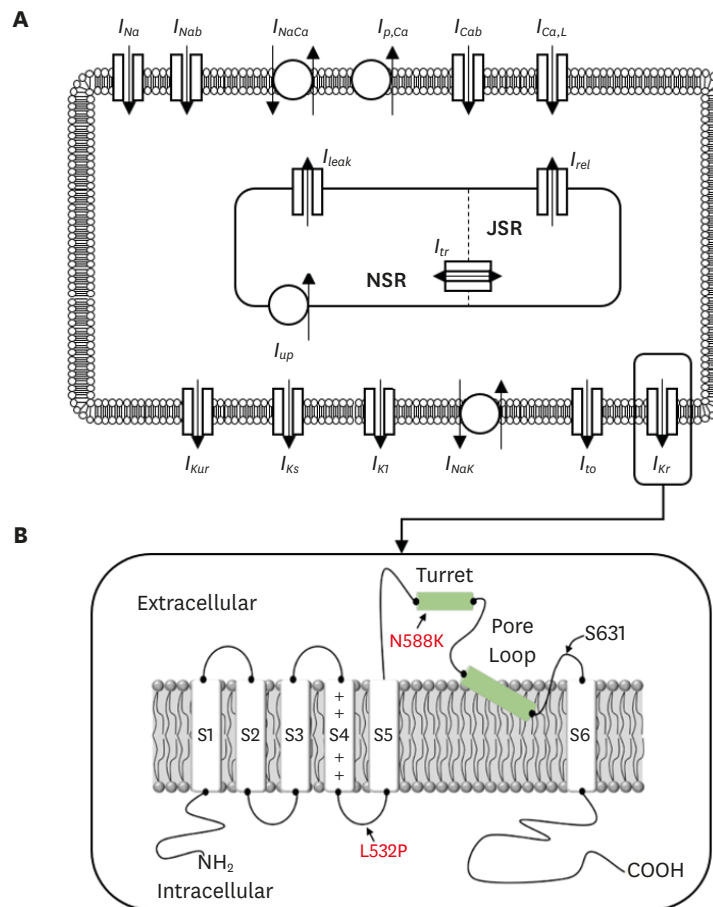
Fig. 1. CRN cell model diagram (**A**), N588K and L532P mutations in the S5 sub-unit of the I_{Kr} channel and in the S4 voltage sensor, respectively (**B**).
CRN = Courtemanche-Ramirez-Nattel.

from the N588K in the *KCNH2* and exhibited Kinect difference due to complex temperature dependency. Changes in the *KCNH2* ion channel due to these mutations cause sudden cardiac death, resulting in abnormal QT intervals on the ECG.[14] Therefore, it is essential to understand their association with cardiac arrhythmia through experiments related to *KCNH2* ion channels.

The experimental measurement of *KCNH2* ion channels is time-intensive and expensive. Hence, researchers have observed the effects of a few mutations on the action potential duration (APD) and the propagation signal in a simulation study using advanced cardiac electrophysiology in three-dimensional (3D) heart models. In 2012, Adeniran et al.[15] performed a simulation to study the effect of the D172N mutation on the APD, ECG, and the electrical propagation signal in 3D ventricles. In 2014 and 2016, our group studied the relation of two mutations (V241F and G229D) with atrial arrhythmia using methods similar to those used by Adeniran et al.[16,17] In previous studies, simulations of the *KCNH2* mutations— N588K and L532P—have been limited to a single cell model and a two-dimensional (2D) tissue model. Thus, quantification of the electric conduction patterns in the 3D heart geometry is limited. Therefore, in this study, we enhanced the observation of atrial conduction patterns due to *KCNH2* ion channel mutation by applying the L532P and N588K mutations to the 3D atrium model as well. We hypothesize that L532P mutation plays a role in atrial fibrillation (AF) generation due to the significant shortening of APD by the mutation.

To simulate the AF conditions, we used Courtemanche-Ramirez-Nattel (CRN) electrophysiological model to simulate the WT, L532P, and N588K mutation conditions. The experimental values for the I_{Kr} mutation measured in previous studies were applied to the CRN cell model, and N588K and L532P mutation. The proarrhythmic effect of the *KCNH2* ion channel variation was analyzed by comparing the differences in the APD, current density of I_{Kr}, wavelength, electrical activation in 2D and 3D geometry, and a vulnerable window between the wildtype (WT) and mutated (MT) genes.

METHODS

To numerically simulate the electrical excitation of the cell, a model of cellular voltage change caused by the flux of ions (Na^+, K^+, Ca^{2+}, Cl^-) in and out of the cell is required. Electrical equilibrium (Hodgkin and Huxley[18]) is used to describe the changes in intracellular voltage when the bio-electrons entering the cell are injected into or out of the cell.

$$C_m \frac{dV_m}{dt} = -(I_{ion} + I_{stim}) \tag{1}$$

In (1), C_m is cell membrane capacitance per unit cell and V_m is cell voltage. I_{ion} is the total bio-ion current flowing into the cell, and I_{stim} is the amount of perturbation current flowing in and out of the cell to induce excitation of the cell. I_{ion} varies slightly depending on the cell model and channel type.

In this study, we used the CRN (**Fig. 1A**) model for the human atrium cell model. Similar to the Hodgkin and Huxley model, the CRN modeled the cell membrane as a capacitor connected with variable resistances (ionic channels) and batteries (driving forces) in parallel.[19] The ionic channels (I_{ion}) of the CRN model are as follows:

$$I_{ion,atrium} = I_{Na} + I_{K1} + I_{to} + I_{Kur} + I_{Kr} + I_{Ks} +$$
$$I_{Ca,L} + I_{p,Ca} + I_{NaCa} + I_{b,Na} + I_{b,Ca} \tag{2}$$

In (2), I_{Na} represents rapid inward Na$^+$ current, I_{K1} is inward rectifier K$^+$ current, I_{to} is transient outward K$^+$ current, I_{Kur} is ultra-rapid delayed rectifier K$^+$ current, I_{Kr} is rapid delayed rectifier K$^+$ current, I_{Ks} is slow delayed rectifier K$^+$ current, $I_{Ca,L}$ is L-type inward Ca^{2+} current, $I_{p,Ca}$ is plateau current, I_{NaCa} is Na$^+$/Ca^{2+} exchanger current, and $I_{b,Na}$, and $I_{b,Ca}$ are background Na$^+$ and Ca^{2+} currents, respectively. Details of this have been described in previous studies.[19] We used the CRN model in this study because the mathematical equations of the L532P and N588K mutations were measured and calibrated to be fit with the CRN model. Moreover, it is a well-known electrophysiological model for human atrial cells.

Modified CRN cell model

We modified some ion currents to mimic closely related AF phenomena following Jacquemet et al.[20] The modified model reduces the I_{to}, I_{CaL}, and I_{kur} currents by 80%, 30%, and 90%, respectively, and increases the I_{Kr} by 50%, resulting in AF action potential similar to the actual clinical results. We compared the original parameter input of CRN with the modified parameter of that in Jacquemet et al.[20] study at the single-cell level (**Fig. 2**). In the 2D tissue and 3D atrium, we presented the electrophysiological activation based on the modified parameters setting.

Implementation of mutation

The I_{Kr} of the CRN model was modified to accommodate I_{Kr} changes due to gene mutation (**Fig. 1B**). For this, maximal I_{Kr} conductance, activation, and inactivation gate values, and α- and β-subunit values of the CRN model were substituted into the gene mutation experimental values measured in the previous studies.[13,21,22] The L532P mutation was applied to Xenopus laevis oocytes using a double-electrode voltage-clamp assay (Hassel et al.[13]), and the N588K mutation was examined in Chinese hamster ovary cell counts measured at room temperature, 37°C (McPate et al.[21]). CRN models using N588K gene mutations in I_{Kr} have been described by Loewe et al.[22] and assumes the following explanation:

$$I_{K,r} = P_1 x_{r1} x_{r2} (V_m - E_K) \tag{3}$$

$$x_{r2} = \left[1 + exp\left(\frac{V_m + P_2}{P_3}\right)\right] \tag{4}$$

$$\frac{dx_{r1}}{dt} = \frac{x_{r1\infty} - x_1}{\tau_{x_{r1}}} \tag{5}$$

$$x_{r1\infty} = \left[1 + exp\left(\frac{-(V_m + P_4)}{P_5}\right)\right] \tag{6}$$

$$\alpha_{x_{r1}} = P_6 \frac{V_m + P_7}{1 - exp\left(\frac{V_m + P_7}{P_8}\right)} \tag{7}$$

$$\beta_{x_{r1}} = 7.3898 \times 10^{-5} \frac{V_m + P_9}{exp\left(\frac{V_m + P_9}{P_{10}}\right) - 1} \tag{8}$$

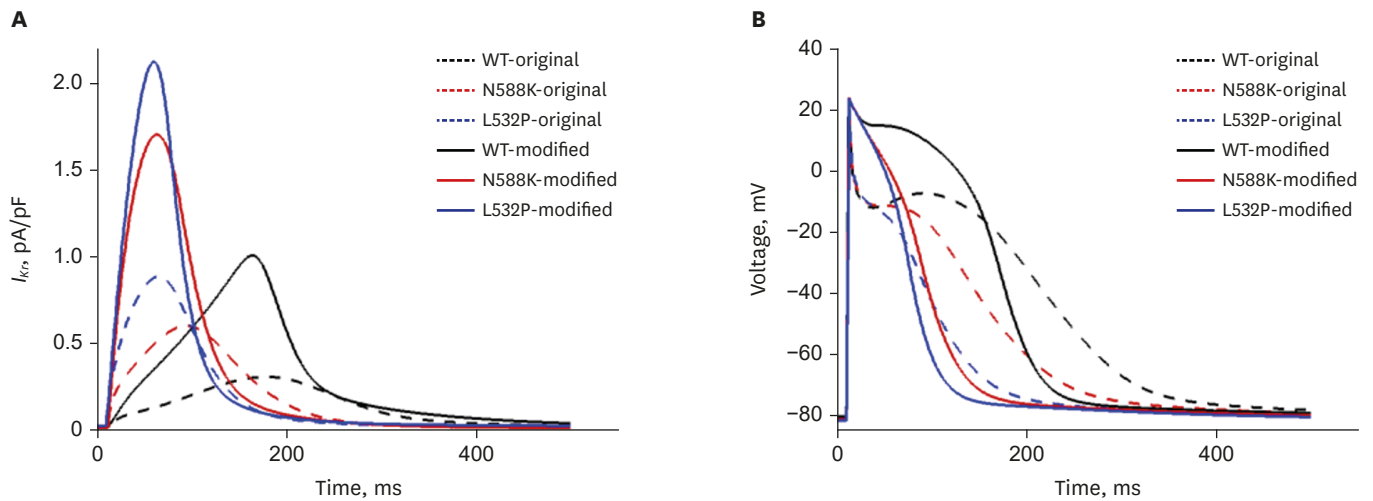$$\tau_{x_{r1}} = [(\alpha_{x_{r1}} + \beta_{x_{r1}}) \cdot P_{11}] \tag{9}$$

Fig. 2. I_{kr} current profiles (**A**), Action potential (**B**).

In (3), I_{Kr} is rapid delayed outward rectifier K⁺ current, and *xr1* in (4) and *xr2* in (5) are the activation and inactivation gating variables, respectively. *αxr1* in (7) and *βxr1* in (8) are the forward and backward rate constants for the gating variable, and *τxr1* in (9) is the time constant for gating variables. P1-11 are experimental values for WT, N588K, and L532P mutation conditions (the values of P1-11 are provided in **Table 1**).[22]

Tissue model

In 2D models, the spatial resolution was 0.02 cm; this is comparable to the size of atrial cells and provides a stable numerical solution. The size of the 2D atrial sheet model was 10 × 10 cm². The number of nodes and elements was 250,000 and 249,001, respectively. The purpose of the 2D simulation is to present the electrophysiological activation pattern of both N588K & L532P mutations on a simplified and limited medium. The limited 2D medium can show the arrhythmogenic and the duration of the rotor. The pattern shown can provide some clues of what happens in the 3D heart which is more complex geometry. The mesh of the 3D atrium is shown in **Fig. 3**. The electrophysiological model of the cardiac tissue was based on the following equation:

Table 1. Parameter values of the control and mutation condition

Variables	Control	N588K	L532P
g_{Kr}			
$\quad P_1$, nS/pF	0.029412	0.029412	0.09172
Inactivation			
$\quad P_2$, mV	15	−38.65	−15.54
$\quad P_3$, mV	22.4	19.46	24.37
Activation			
$\quad P_4$, mV	14.1	16.49	−9.88
$\quad P_5$, mV	6.5	6.76	22.31
A			
$\quad P_6$, 1/mVmsec	0.0003	0.0003	0.00025
$\quad P_7$, mV	14.1	14.1	−196.86
$\quad P_8$, mV	−5	−5	−131.36
B			
$\quad P_9$, mV	−3.3328	−3.3328	−40
$\quad P_{10}$, mV	5.1237	5.1237	3.79 × 10⁻⁶
KQ10			
$\quad P_{11}$, 1	1	2	1

The parameters were obtained based on the experimental data from the work of Loewe et al.[22]

Initial stimulus (S1)
from the SA node

No. of nodes: 205,444
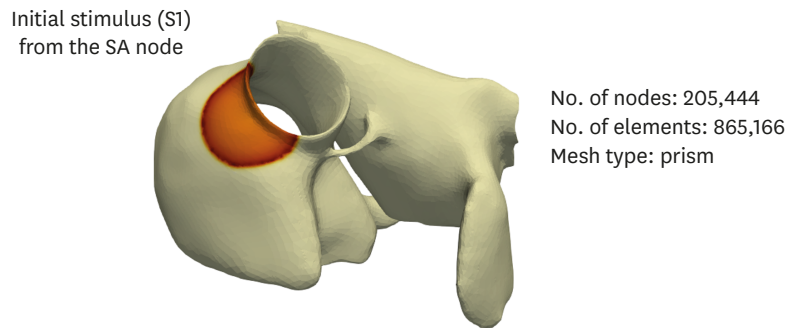No. of elements: 865,166
Mesh type: prism

Fig. 3. Mesh of the 3D atrial model.

$$\frac{\partial V_m}{\partial t} = \frac{1}{\beta C_m} \nabla \cdot D \nabla V_m - \frac{1}{C_m}(I_{ion}(V_m, \vec{n}) - I_{ext}) \tag{10}$$

where V_m represents membrane voltage, t represents time, D is the diffusion coefficient of the tissue, C_m indicates membrane capacitance, I_{ion} is the sum of all transmembrane ionic currents, $\vec{n}$ is the activation gate variable, and I_{ext} is the externally applied stimulus. The partial differential equation above represents electrical propagation in the cardiac tissue; it covers diffusion in the tissue, and reaction in cardiac channels. The parameter values of the above equations are shown in **Table 2**.

Computational resource

The hardware that we used for the simulation is a super-computer which consists of 12 processor units divided into two sockets. Each socket has 16 Gb memory so the total memory is 32 Gb with 6 cores in each socket. The processor series is Intel(R) Xeon(R) CPU E5-26400. Each core handles 1 thread per run. The operating system of the computer is CentOS Linux distribution with kernel version 2.6.18-238.3l5. The code to run the simulation is based on the C++ with Portable, Extensible Toolkit for Scientific Computation (PETSc) library for parallel computing.

Table 2. Parameter values of the current model

Symbols	Description	Values	Unit
C_m	Total membrane capacitance	1	uF/cm²
D	Diffusion coefficient of tissue	0.0001	cm²/msec
F	Faraday constant	96.4867	C/mmol
R	Ideal gas constant	8.3143	J/K/mol
T	Absolute temperature	310	K
g_{Na}	Maximal I_{Na} conductance	7.8	nS/pF
g_{K1}	Maximal I_{K1} conductance	0.09	nS/pF
g_{to}	Maximal I_{to} conductance	0.1652	nS/pF
g_{Kr}	Maximal I_{Kr} conductance	0.0294	nS/pF
g_{Ks}	Maximal I_{Ks} conductance	0.129	nS/pF
$g_{Ca,L}$	Maximal $I_{Ca,L}$ conductance	0.1238	nS/pF
$g_{b,Ca}$	Maximal $I_{b,Ca}$ conductance	0.00113	nS/pF
$g_{b,Na}$	Maximal $I_{b,Na}$ conductance	0.000674	nS/pF
$I_{NaK,max}$	Maximal I_{NaK}	0.6	pA/pF
$I_{NaCa,max}$	Maximal I_{NaCa}	1,600	pA/pF
$I_{p,Ca,max}$	Maximal $I_{p,Ca}$	0.275	pA/pF
$I_{up,max}$	Maximal I_{up}	0.005	mmol/msec

Simulation protocol

We conducted single-cell simulations of MT and WT conditions with original parameters of CRN and modified maximum conduction values (as mentioned in part A) before performing the 2D and 3D simulation. Single-cell action potential was computed by conditioning the cell models for 30 times, at a basic cycle length (BCL) of 1 seconds with supra-threshold stimuli of 1.5 nA/pF (duration of 2 msec). APD90 was defined as the duration between action potential upstroke and 90% repolarization (−71 mV for CRN model). Diastolic interval (DI) was defined as the time interval between 90% repolarization of the previous action potential and the upstroke of an action potential.

Single atrial cell models have then incorporated into a multicellular 2D sheet and 3D models using simplified homogenous electrophysiology of the human atria. Re-entrant waves in the 2D and 3D models were initiated using a standard S1-S2 protocol. S1-S2 protocol is a common protocol to artificially trigger reentry generation, hence arrhythmia.[23-25] The reentry occurrence will lead to spiral wave generation (in 2D tissue) and scroll wave (in 3D geometry) depending on the wavelength, conduction velocity, medium, and the effective refractory period. In the 2D model, three S1 stimuli were applied in sequence every 400 msec to produce a planar wave-front propagating in one direction. After allowing four planar waves to pass, a premature stimulus was applied in the lower left quadrant of the patch. **Fig. 4A** describes the principle of the S1-S2 protocol used in the 2D model (**Fig. 4A**).

In the 3D model, three S1 stimuli were applied in the SA node (**Fig. 4B**). When the refractory tail of this wave reached the center of the medium, and S2 stimulus was applied, parallel with the S1 stimulus, but cover only three-quarters of the length of the medium. This produced a second wavefront with a curly tip, generating a spiral wave. Temporal time-lapse was recorded as 0.05 msec for both 2D and 3D simulations.
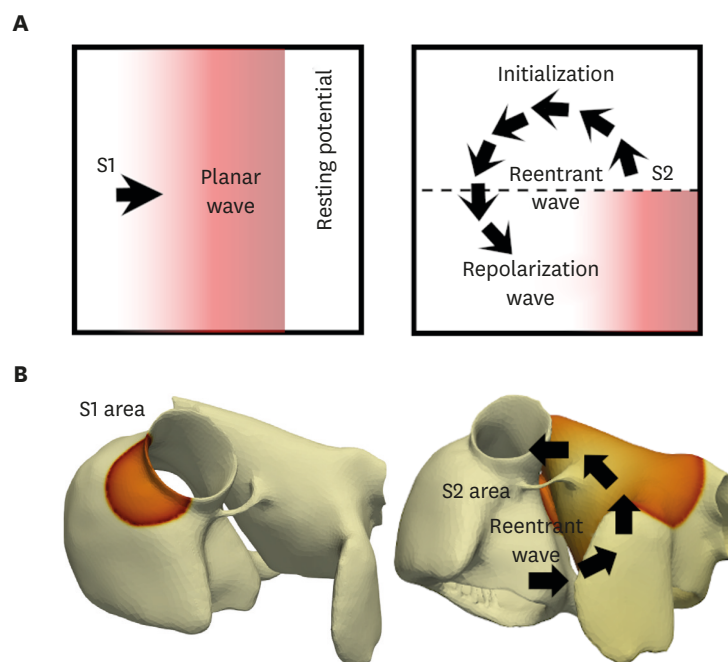
Fig. 4. Description of the S1-S2 protocol in the 2D (**A**) and 3D (**B**) models.

To reveal the vulnerable time window under MT and WT conditions, we conducted periodic stimulation for all cases by using 3D heart tissue. First, we applied 10-fold of stimuli at the apex to create planar waves from apex to the base with 600 msec cycle length. Then we applied the 11th stimulation periodically in ranged from 450 msec to 150 msec with 10 msec decrease. These methods reveal the vulnerable window which generates reentry, thus arrhythmia, under N588K, L532P, and WT conditions.

RESULTS

The comparison of the action potential and I_{Kr} current between original parameters of CRN and modified CRN with the WT and MT (N588K, L532P) genes is shown in **Fig. 2**. The maximum amplitude of I_{Kr} current was 1.003, 1.703, and 2.125 (pA/pF) for WT, N588K, and L532P, respectively, and MT showed a greater increase than WT. Also, the current peak time of I_{Kr} reached 163.4, 63.6, and 60 (msec) for WT, N588K, and L532P, respectively. For APD90, MT reached its peak value earlier than WT (214.4 msec for WT, 104.99 msec for N588K, 105.26 msec for L532P) with the APD50 of 160.6, 76.8, and 63.2 msec for WT, N588K, and L532P, respectively (**Table 3**).

The re-entrant wave pattern of the WT and MT through 2D simulation is presented in **Fig. 5**.

Table 3. Comparison of action potential and I_{Kr} current results between the original and modified crn cell models (WT, N588K, L532P)

| Variables	Original CRN cell model					Modified CRN cell model				
	Action potential			I_{Kr} current		Action potential			I_{Kr} current	
	Amplitude	APD$_{90}$	APD$_{50}$	$I_{Kr,max}$	t($I_{Kr,max}$)	Amplitude	APD$_{90}$	APD$_{50}$	$I_{Kr,max}$	t($I_{Kr,max}$)
WT	100.41	308.0	184.9	0.298	179.2	95.49	214.4	160.6	1.003	163.4
N588K	101.75	236.4	116.5	0.593	95.0	104.99	135.9	76.8	1.703	63.6
L532P	102.95	160.5	71.1	0.880	66.0	105.26	111.8	63.2	2.125	60.0

APD = action potential duration, CRN = Courtemanche-Ramirez-Nattel, I_{Kr} = rapid delayed rectifier potassium channel, t = time, WT = wildtype.
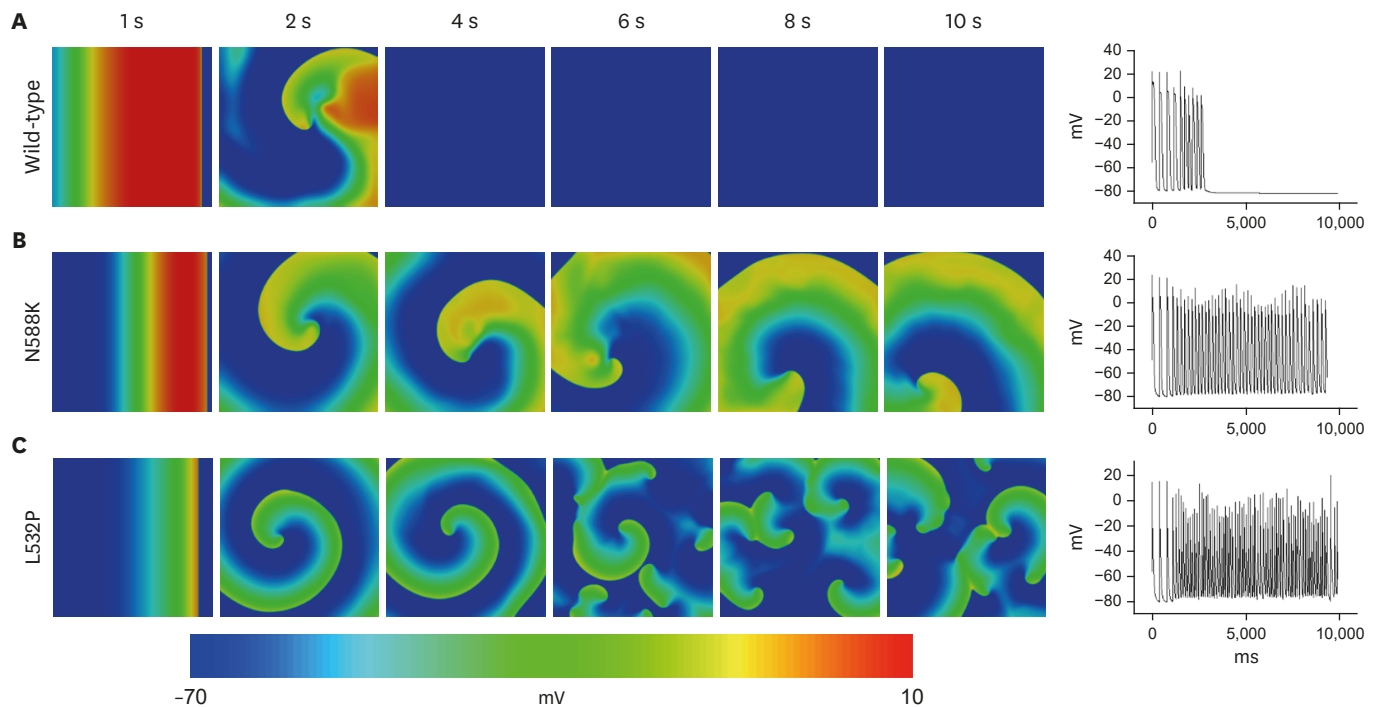

Fig. 5. Spiral wave activity and action potential shape observed in the 2D tissue model. WT (**A**), N588K mutation (**B**), and L532P mutation (**C**).

In contrast to self-termination without wave breakup after 2,000 msec from the start of the last S1 stimulus (**Fig. 5A**), MTs maintained non-termination during the simulation period. The N588K mutation maintained a stable reentrant wave for 10 seconds (**Fig. 5B**), whereas the L532P mutation had a wave breakup after 3,300 msec from the start of the last S1 stimulus and a fibrillation phenomenon where the waveform split into smaller fragments (**Fig. 5C**).

The results of the electrical conduction simulation of the WT and MT for the 3D atrial model are shown in **Fig. 6**. The wavelengths were in the order of WT ≥ N588K > L532P and the
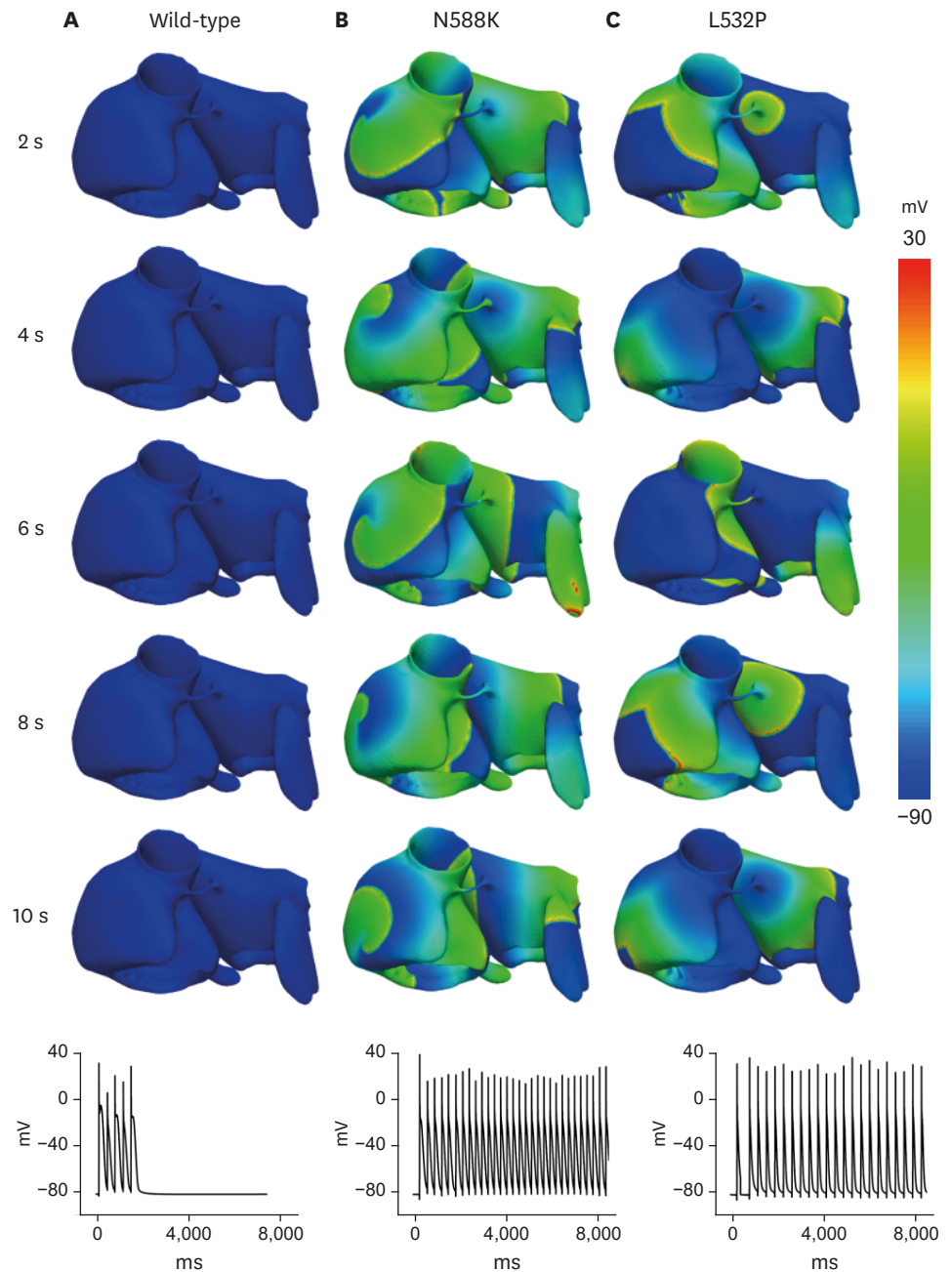
Fig. 6. Spiral wave activity and action potential shape observed in the 3D atrial model. WT (**A**), N588K mutation (**B**), and L532P mutation (**C**).
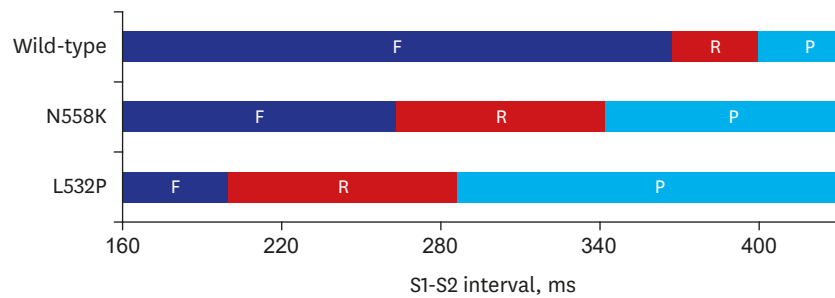
Fig. 7. "Vulnerability to re-entry" grid constructed by summarizing the outcomes at varying S10th and S11th intervals. F = failure to initiate S11th stimulus, P = normal propagation of S2 beat, R = re-entry.

conduction velocities for all three were similar (19.7 cm/sec ± 0.2 cm/sec). As a result of the spiral wave characteristics, the WT was self-terminate at 2 seconds after the S2 stimulus with a rather unstable re-entrant wave (**Fig. 6A**). In the N588K, a stable re-entrant wave was maintained until the end of the simulation after the S2 stimulus (**Fig. 6B**). In the L532P, the re-entrant wave progressed and a wave breakup phenomenon occurred generating an irregular waveform (**Fig. 6C**).

The vulnerable window of the WT and MT according to the 10th stimuli and 11th stimuli interval in the 3D LA model is shown in **Fig. 7**. The interval of the 10th and 11th stimuli was between 150 msec to 450 msec with a 10 msec resolution. The red block with F indicates the failure to generate an electrical signal in the tissue by the 11th stimulus due to the effective refractory period. The yellow block with R indicates that re-entry occurs by the 11th stimulus within that time interval. The re-entry interval in WT ranged from 360 msec to 400 msec. The re-entry interval in N588K and L532P were 270 msec to 340 msec and 200 msec to 290 msec, respectively. Lastly, the blue block with the letter P indicates a normal planar wave propagation of an electrical signal by the 11th stimulus.

DISCUSSION

In this study, we simulated *KCNH2* mutations using an electrophysiological 3D atrial model. To this end, we modified two aspects of the CRN cell model. First, we modified the ion currents presented in a previous study and applied them to our cell model.[20] Second, the clinical data of N588K and L532P mutations derived from previous studies were assigned to our cell model.[13,21] This modified cell model for the mutation described by Loewe et al.[22] was then applied to the anatomical LA model provided by Yonsei Severance Hospital to observe the *KCNH2* mutation phenomenon.

First, the effect of the modified CRN cell model was confirmed by measuring I_{Kr} current (**Fig. 4A**) and AP (**Fig. 4B**). The maximum amplitude of I_{Kr} current in MT conditions was higher than that in the original CRN model, and it was observed earlier than the original CRN model. This change in I_{Kr} due to MT conditions resulted in a shortening of the APD, which further resulted in APD50 and APD90 being shorter than that of the CRN model. This confirmed that the modified ion current shortens the APD of the CRN model (**Table 3**). Shortening of the APD is important to induce fibrillation by increasing the vulnerability of the 2D and 3D models, indicating that the modified CRN cell model can exhibit fibrillation condition realistically.

The application of *KCNH2* mutation to the modified cell model confirmed that the N588K and L532P mutations advance the peak I_{Kr} current and maximize the amplitude (**Table 3**). This change in I_{Kr} causes early repolarization, shortens the plateau of the AP compared to the normal condition, and ultimately shortens the APD. This suggests a relationship between *KCNH2* mutations and the short QT syndrome, and comprehensively explains the increase in tissue susceptibility that maintains and sustains re-entry.

In this study, we analyzed the 2D tissue and 3D LA models by applying the N588K and L532P mutations to the modified cell model and confirmed that vulnerability is increased by the mutation. For the WT, the spiral wave is self-terminated due to the long wavelength that results in the lack of sufficient space for activation in the tissue. However, the N588K and L532P mutations significantly shortened the wavelength, which allows the spiral wave to remain constant. Previous studies have shown that the N588K-hERG SQT1 mutation in 2D and 3D tissues can reduce the minimum substrate size to allow for re-entry.[26] These results were confirmed by the N588K mutation effect in this study. In particular, the L532P mutation was found to cause a wave break-up phenomenon after a time-lapse, resulting in irregular conduction-sustaining fibrillation. This confirmed our hypothesis that due to the significant APD shortening by the L532P, the electrical pattern wave propagates in such a chaotic condition resulting in the spiral wave break up (AF condition). The impact of the *KCNH2* mutation on the vulnerability of the atrium model is also confirmed by a vulnerability graph in **Fig. 7**. Re-entrant waves were generated within 40 msec for WT, whereas for the N588K and L532P mutations, they were generated within 80 and 100 msec, respectively. This suggests that the effect of MT increases the vulnerability of the atrium model and that *KCNH2* mutation causes AF.

Researchers have reported pharmacological substances that blockade the I_{Kr} channel, hence prolonged the QT interval including Vesnarione,[27] Macrolide Antibiotic,[28] Ketoconazole,[29] and Seldane.[30] However, none of the studies specifically observed the effect of the I_{Kr} blocker on either N588K or L532P mutation conditions. In 2004, Brugada et al.[6] attempted to apply Sotalol, I_{Kr} blocker, which is categorized as class III antiarrhythmic drugs on N588K-hERG mutation. They found that the N588K mutation decreased the effect of Sotalol on the hERG channel which is consistent with clinical findings. In addition, a proper drug for L532P was open for future pharmacological study.[10]

The limitations of this study are as follows; First, we used a homogeneous cell model as 2D and 3D heart models, however, in reality, the heart tissues are discrete. Second, we only provide the electrophysiological analysis of the two mutations without considering the mechanical behavior, which previously observed for D172N, G229D, S140G, and V241F mutations.[25,31-33] Third, we were unable to compare our simulation results with experimental data due to the limited availability of patients with N588K or L532P mutations. Nonetheless, this computational study demonstrated the relationship between the L532P and N588K mutations with atrial arrhythmia and AF. This study provides further insights into the N588K and L532P mutations to pharmacologists. Patients with N588K or L532P mutations can benefit from drug therapy with appropriate substance and dosage.[34]

In summary, we confirmed that the vulnerability of the atria is increased due to *KCNH2* gene mutations, and the re-entrant wave is constantly maintained throughout the 3D left atrial model. In particular, the CRN modified cell model confirmed that the L532P gene mutation can cause AF.

REFERENCES

1. Hsiao PY, Tien HC, Lo CP, Juang JM, Wang YH, Sung RJ. Gene mutations in cardiac arrhythmias: a review of recent evidence in ion channelopathies. *Appl Clin Genet* 2013;6:1-13.
   PUBMED

2. Wilde AA, Bezzina CR. Genetics of cardiac arrhythmias. *Heart* 2005;91(10):1352-8.
   PUBMED | CROSSREF

3. Chen PS, Garfinkel A, Weiss JN, Karagueuzian HS; CHEN PS. Garfinkel A, Weiss JN, Karagueuzian HS. Spirals, chaos, and new mechanisms of wave propagation. *Pacing Clin Electrophysiol* 1997;20(2):414-21.
   CROSSREF

4. Kannel WB, Benjamin EJ. Status of the epidemiology of atrial fibrillation. *Med Clin North Am* 2008;92(1):17-40.
   PUBMED | CROSSREF

5. Stewart S, Hart CL, Hole DJ, McMurray JJ. A population-based study of the long-term risks associated with atrial fibrillation: 20-year follow-up of the Renfrew/Paisley study. *Am J Med* 2002;113(5):359-64.
   PUBMED | CROSSREF

6. Brugada R, Hong K, Dumaine R, Cordeiro J, Gaita F, Borggrefe M, et al. Sudden death associated with short-QT syndrome linked to mutations in HERG. *Circulation* 2004;109(1):30-5.
   PUBMED | CROSSREF

7. Gussak I, Brugada P, Brugada J, Wright RS, Kopecky SL, Chaitman BR, et al. Idiopathic short QT interval: a new clinical syndrome? *Cardiology* 2000;94(2):99-102.
   PUBMED | CROSSREF

8. Giustetto C, Di Monte F, Wolpert C, Borggrefe M, Schimpf R, Sbragia P, et al. Short QT syndrome: clinical findings and diagnostic-therapeutic implications. *Eur Heart J* 2006;27(20):2440-7.
   PUBMED | CROSSREF

9. Hong K, Bjerregaard P, Gussak I, Brugada R. Short QT syndrome and atrial fibrillation caused by mutation in KCNH2. *J Cardiovasc Electrophysiol* 2005;16(4):394-6.
   PUBMED | CROSSREF

10. Zhang YH, Colenso CK, Sessions RB, Dempsey CE, Hancox JC. The hERG K(+) channel S4 domain L532P mutation: characterization at 37°C. *Biochim Biophys Acta* 2011;1808(10):2477-87.
    PUBMED | CROSSREF

11. Sanguinetti MC, Jiang C, Curran ME, Keating MT. A mechanistic link between an inherited and an acquired cardiac arrhythmia: HERG encodes the IKr potassium channel. *Cell* 1995;81(2):299-307.
    PUBMED | CROSSREF

12. Trudeau MC, Warmke JW, Ganetzky B, Robertson GA. HERG, a human inward rectifier in the voltage-gated potassium channel family. *Science* 1995;269(5220):92-5.
    PUBMED | CROSSREF

13. Hassel D, Scholz EP, Trano N, Friedrich O, Just S, Meder B, et al. CLINICAL PERSPECTIVE. *Circulation* 2008;117(7):866-75.
    PUBMED | CROSSREF

14. Vandenberg JI, Walker BD, Campbell TJ. HERG K+ channels: friend and foe. *Trends Pharmacol Sci* 2001;22(5):240-6.
    PUBMED | CROSSREF

15. Adeniran I, El Harchi A, Hancox JC, Zhang H. Proarrhythmia in KCNJ2-linked short QT syndrome: insights from modelling. *Cardiovasc Res* 2012;94(1):66-76.
    PUBMED | CROSSREF

16. Imaniastuti R, Lee HS, Kim N, Youm JB, Shim EB, Lim KM. Computational prediction of proarrhythmogenic effect of the V241F KCNQ1 mutation in human atrium. *Prog Biophys Mol Biol* 2014;116(1):70-5.
    PUBMED | CROSSREF

17. Zulfa I, Shim EB, Song KS, Lim KM. Computational simulations of the effects of the G229D KCNQ1 mutation on human atrial fibrillation. *J Physiol Sci* 2016;66(5):407-15.
    PUBMED | CROSSREF

18. Hodgkin AL, Huxley AF. A quantitative description of membrane current and its application to conduction and excitation in nerve. *J Physiol* 1952;117(4):500-44.
    PUBMED | CROSSREF

19. Courtemanche M, Ramirez RJ, Nattel S. Ionic mechanisms underlying human atrial action potential properties: insights from a mathematical model. *Am J Physiol* 1998;275(1):H301-21.
    PUBMED

20. Jacquemet V, Virag N, Ihara Z, Dang L, Blanc O, Zozor S, et al. Study of unipolar electrogram morphology in a computer model of atrial fibrillation. *J Cardiovasc Electrophysiol* 2003;14(10 Suppl):S172-9.
    PUBMED | CROSSREF

21. McPate MJ, Duncan RS, Milnes JT, Witchel HJ, Hancox JC. The N588K-HERG K+ channel mutation in the 'short QT syndrome': mechanism of gain-in-function determined at 37 degrees C. *Biochem Biophys Res Commun* 2005;334(2):441-9.
    PUBMED | CROSSREF

22. Loewe A, Wilhelms M, Fischer F, Scholz EP, Dössel O, Seemann G. Arrhythmic potency of human ether-a-go-go-related gene mutations L532P and N588K in a computational model of human atrial myocytes. *Europace* 2014;16(3):435-43.
    PUBMED | CROSSREF

23. Hwang M, Kwon SS, Wi J, Park M, Lee HS, Park JS, et al. Virtual ablation for atrial fibrillation in personalized in-silico three-dimensional left atrial modeling: comparison with clinical catheter ablation. *Prog Biophys Mol Biol* 2014;116(1):40-7.
    PUBMED | CROSSREF

24. Xie F, Qu Z, Yang J, Baher A, Weiss JN, Garfinkel A. A simulation study of the effects of cardiac anatomy in ventricular fibrillation. *J Clin Invest* 2004;113(5):686-93.
    PUBMED

25. Jeong DU, Lim KM. Influence of the KCNQ1 S140G mutation on human ventricular arrhythmogenesis and pumping performance: simulation study. *Front Physiol* 2018;9:926.
    PUBMED | CROSSREF

26. Adeniran I, Hancox JC, Zhang H. In silico investigation of the short QT syndrome, using human ventricle models incorporating electromechanical coupling. *Front Physiol* 2013;4:166.
    PUBMED | CROSSREF

27. Kamiya K, Mitcheson JS, Yasui K, Kodama I, Sanguinetti MC. Open channel block of HERG K(+) channels by vesnarinone. *Mol Pharmacol* 2001;60(2):244-53.
    PUBMED | CROSSREF

28. Volberg WA, Koci BJ, Su W, Lin J, Zhou J. Blockade of human cardiac potassium channel human ether-a-go-go-related gene (HERG) by macrolide antibiotics. *J Pharmacol Exp Ther* 2002;302(1):320-7.
    PUBMED | CROSSREF

29. Dumaine R, Roy ML, Brown AM. Blockade of HERG and Kv1.5 by ketoconazole. *J Pharmacol Exp Ther* 1998;286(2):727-35.
    PUBMED

30. Roy M, Dumaine R, Brown AM. HERG, a primary human ventricular target of the nonsedating antihistamine terfenadine. *Circulation* 1996;94(4):817-23.
    PUBMED | CROSSREF

31. Heikhmakhtiar AK, Rasyidin FA, Lim KM. V241F KCNQ1 mutation shortens electrical wavelength and reduces ventricular pumping capabilities: a simulation study with an electro-mechanical model. *Front Phys* 2018;6:147.
    CROSSREF

32. Yuniarti AR, Setianto F, Marcellinus A, Hwang HJ, Choi SW, Trayanova N, et al. Effect of KCNQ1 G229D mutation on cardiac pumping efficacy and reentrant dynamics in ventricles: computational study. *Int J Numer Methods Biomed Eng* 2018;34(6):e2970.
    PUBMED | CROSSREF

33. Heikhmakhtiar AK, Lee CH, Song KS, Lim KM. Computational prediction of the effect of D172N KCNJ2 mutation on ventricular pumping during sinus rhythm and reentry. *Med Biol Eng Comput* 2020;58(5):977-90.
    PUBMED | CROSSREF

34. Tamargo J, Caballero R, Gómez R, Valenzuela C, Delpón E. Pharmacology of cardiac potassium channels. *Cardiovasc Res* 2004;62(1):9-33.
    PUBMED | CROSSREF